

Fig. 9. Effect of Amino Acid and Organic Acid Combinations on the Activity of Freeze-Dried Lactate Dehydrogenase (50 $\mu\text{g}/\text{ml}$, Average \pm S.D., $n=3$)

nine freeze-dried with inorganic acids (e.g., HCl, H_3PO_4).¹³ A carboxyl group band at 1725 cm^{-1} appeared when the citric acid ratio was increased. Diffuse-reflection near-infrared spectra obtained non-destructively at the bottom of the glass vials also indicated the altered local environment of the functional groups. A large amino band of L-arginine (6505 cm^{-1} , N-H stretching 1st overtone) disappeared in the presence of lower molar concentration ratio of citric acid in the initial solution (140 mM L-arginine, 60 mM citric acid). Increasing the citric acid ratio also reduced the large absorption band at 4920 cm^{-1} , and concomitantly induced band at 5030 cm^{-1} in the co-lyophilized solids. Assignment of these bands remains to be elucidated. The results strongly suggested hydrogen-bonding and/or electrostatic interactions between L-arginine and citric acid in the lyophilized solids.

Effect of Excipients on Inactivation of Freeze-Dried LDH Freeze-drying of LDH in the absence of the stabilizing excipients resulted in significant reduction of the activity (approximately 15% of the initial solution) (Fig. 9). Higher enzyme activity was retained in freeze-drying at a higher phosphate buffer concentration (50 mM). Some amino acid and organic acid combinations that provide neutral to weakly acidic initial solution (pH 5–8) and amorphous dried solids also retained the enzyme activity. The enzyme lost most of the activity in freeze-drying from extreme pH solutions (e.g., 200 mM L-arginine, pH 10.6). Addition of citric acid or L-tartaric acid slightly reduced the effect of L-histidine to retain the activity of LDH during freeze-drying. Crystallization of glycine in the single-solute frozen solution, and concomitant loss of the protecting effect, should explain the lower remaining enzyme activity.^{1,2,22}

Discussion

The freeze-drying of aqueous solutions containing some basic or neutral amino acid (e.g., L-arginine, L-histidine) and hydroxy di- or tricarboxylic acid (e.g., citric acid, L-tartaric acid) combinations resulted in the glass-state amorphous solid cakes that protect proteins from dehydration stresses. Some of the solids showed glass transition temperatures comparable to those of disaccharides (e.g., sucrose, trehalose).⁴ The data and recent literature on the properties of related substances in different physical states (e.g., complex

crystals, ionic liquids) strongly suggested contribution of the multiple functional groups of the consisting molecules to form the interaction (e.g., electrostatic, hydrogen-bonding) networks required for the glass-state amorphous solids.^{23–25} Multiple amino, carboxyl, and hydroxyl groups in the solute molecules raise transition temperatures of the mixture frozen solutions (T'_g) and the freeze-dried solids (T_g).¹⁵ The ammonium carbohydrate ion pairs form multiple hydrogen-bondings in some non-polar solvents.^{23,24} Differently protonated carboxyl and carboxylate groups also form an intermolecular hydrogen-bonding network.²⁵

The amino acids and organic acids containing plural amino or carboxyl groups should have large chance to form the interactions with multiple counterpart molecules. The contribution of the multiple functional groups should explain the high transition temperatures (T'_g , T_g) of the L-arginine and citric acid combination. L-Arginine also forms stable amorphous freeze-dried solids with multivalent inorganic acids (e.g., H_3PO_4).^{11,13} Frozen sodium citrate and tartrate buffer solutions exhibit the highest T'_g at certain sodium concentration ratios.¹⁷ Supramolecular interactions (e.g., peptide-like periodic interactions) reported in some complex crystals of amino acid and dicarboxylic acid (e.g., L-arginine and adipic acid, X-ray analysis)²⁶ should support the possible multi-molecular interaction network in the less-ordered amorphous phase.

Hydroxyl groups in the citric acid, L-tartaric acid, and DL-malic acid should introduce additional hydrogen bonding to the amorphous phase. The number of hydroxyl groups in the component, and the accompanying change in the molecular interactions are major factors in determining the glass transition temperature of some ionic liquids composed of an amino acid and a 1-allylimidazolium cation.²⁷ The intense interactions and resulting reduction of the molecular mobility may prevent the crystallization of amino acids (e.g., glycine, glutamine) at concentration ratios much lower than those of "inert" nonionic solutes (e.g., sucrose) or inorganic salts (e.g., NaCl).^{17,30–32}

The high glass transition temperature amorphous solids formed by combinations of popular excipients would be a practical alternative to disaccharides in the design of freeze-dried protein formulations. The excipient combinations would satisfy the two major protein-stabilizing mechanisms postulated on saccharides, namely substitution of the surrounding water molecules by hydrogen-bonding and reduction of the chemical reaction by embedding in the glass-state solids.^{6–8} Additional effects of some amino acids (e.g., reduced aggregation in aqueous solution by L-arginine) preferable in protein formulations are also anticipated.⁹ The limited crystallinity and low volatility of the amino acid and organic acid should reduce the risk of pH change and the resulting protein inactivation in the freeze-drying process reported in some buffer systems.²⁸

Various proteins degrade during the freeze-drying process and subsequent storage through several chemical and physical mechanisms.^{3,29} The low concentration LDH solution is often used as a model system for studying the effect of cosolutes in the freeze-thawing and freeze-drying processes because of its apparent tendency to lose its activity due to irreversible subunit dissociation and conformation change.³⁰ The ability of excipient combinations to retain the enzyme

activity in the freeze-drying process should indicate the stabilization of the quarterly structure against freeze-concentration and dehydration stress. Different molecular mobility, local pH, water content, and crystallinity of the excipients may affect the chemical degradation rate of the freeze-dried enzyme in the subsequent storage. The freeze-dried basic amino acid and organic acid combination solids should provide the embedded proteins with unique local environments that are significantly different from those of the nonionic excipients (e.g., saccharides). The structural and chemical stability of proteins in these solids during the freeze-drying process and storage is an intriguing topic that needs further study through various model protein and stress systems.

References

- 1) Nail S. L., Jiang S., Chongprasert S., Knopp S. A., *Pharm. Biotechnol.*, **14**, 281—360 (2002).
- 2) Tang X., Pikal M. J., *Pharm. Res.*, **21**, 191—200 (2004).
- 3) Carpenter J. F., Arakawa T., Crowe J. H., *Dev. Biol. Stand.*, **74**, 225—238 (1992).
- 4) Franks F., *Dev. Biol. Stand.*, **74**, 9—18 (1992).
- 5) Lee J. C., Timasheff S. N., *J. Biol. Chem.*, **256**, 7139—7201 (1981).
- 6) Chang B. S., Randall C., *Cryobiology*, **29**, 632—656 (1992).
- 7) Arakawa T., Timasheff S. N., *Arch. Biochem. Biophys.*, **224**, 169—177 (1983).
- 8) Sane S. U., Wong R., Hsu C. C., *J. Pharm. Sci.*, **93**, 1005—1018 (2004).
- 9) Tsumoto K., Umetsu M., Kumagai I., Ejima D., Philo J. S., Arakawa T., *Biotechnol. Prog.*, **20**, 1301—1308 (2004).
- 10) Osterberg T., Fatouros A., Mikaelsson M., *Pharm. Res.*, **14**, 892—898 (1997).
- 11) Mattern M., Winter G., Kohnert U., Lee G., *Pharm. Dev. Technol.*, **4**, 199—208 (1999).
- 12) Osterberg T., Wadsten T., *Eur. J. Pharm. Sci.*, **8**, 301—308 (1999).
- 13) Izutsu K., Fujimaki Y., Kuwabara A., Aoyagi N., *Int. J. Pharm.*, **301**, 161—169 (2005).
- 14) Li J., Chatterjee K., Medek A., Shalaev E., Zografi G., *J. Pharm. Sci.*, **93**, 697—712 (2004).
- 15) Kadoya S., Izutsu K., Yonemochi E., Terada K., Yomota C., Kawanishi T., *Chem. Pharm. Bull.*, **56**, 821—826 (2008).
- 16) Akers M. J., Milton N., Byrn S. R., Nail S. L., *Pharm. Res.*, **12**, 1457—1461 (1995).
- 17) Shalaev E. Y., Johnson-Elton T. D., Chang L., Pikal M. J., *Pharm. Res.*, **19**, 195—201 (2002).
- 18) Chongprasert S., Knopp S. A., Nail S. L., *J. Pharm. Sci.*, **90**, 1720—1728 (2001).
- 19) Lu Q., Zografi G., *J. Pharm. Sci.*, **86**, 1374—1378 (1997).
- 20) Shamblin S. L., Taylor L. S., Zografi G., *J. Pharm. Sci.*, **87**, 694—701 (1998).
- 21) Yonemochi E., Inoue Y., Buckton G., Moffat A., Oguchi T., Yamamoto K., *Pharm. Res.*, **16**, 835—840 (1999).
- 22) Anchordoquy T. J., Carpenter J. F., *Arch. Biochem. Biophys.*, **332**, 231—238 (1996).
- 23) Sada K., Tani T., Shinkai S., *Synlett*, **2006**, 2364—2374 (2006).
- 24) Yerger E. A., Barrow G. M., *J. Am. Chem. Soc.*, **77**, 6206—6207 (1955).
- 25) Kobayashi N., Naito T., Inabe T., *Bull. Chem. Soc. Jpn.*, **76**, 1351—1362 (2003).
- 26) Roy S., Singh D. D., Vijayan M., *Acta Crystallogr. B*, **61**, 89—95 (2005).
- 27) Fukumoto K., Yoshizawa M., Ohno H., *J. Am. Chem. Soc.*, **127**, 2398—2399 (2005).
- 28) Li J., Guo Y., Zografi G., *Pharm. Res.*, **19**, 20—26 (2002).
- 29) Manning M. C., Patel K., Borchardt R. T., *Pharm. Res.*, **6**, 903—918 (1989).
- 30) Seguro K., Tamiya T., Tsuchiya T., Matsumoto J. J., *Cryobiology*, **27**, 70—79 (1990).

Feasibility of ^{19}F -NMR for Assessing the Molecular Mobility of Flufenamic Acid in Solid Dispersions

Yukio Aso,* Sumie YOSHIOKA, Tamaki MIYAZAKI, and Toru KAWANISHI

National Institute of Health Sciences, 1-18-1 Kamiyoga, Setagaya, Tokyo 158-8501, Japan.

Received September 9, 2008; accepted October 22, 2008; published online October 23, 2008

The purpose of the present study was to clarify the feasibility of ^{19}F -NMR for assessing the molecular mobility of flufenamic acid (FLF) in solid dispersions. Amorphous solid dispersions of FLF containing poly(vinylpyrrolidone) (PVP) or hydroxypropylmethylcellulose (HPMC) were prepared by melting and rapid cooling. Spin-lattice relaxation times (T_1 and $T_{1\rho}$) of FLF fluorine atoms in the solid dispersions were determined at various temperatures (-20 to 150°C). Correlation time (τ_c), which is a measure of rotational molecular mobility, was calculated from the observed T_1 or $T_{1\rho}$ value and that of the T_1 or $T_{1\rho}$ minimum, assuming that the relaxation mechanism of spin-lattice relaxation of FLF fluorine atoms does not change with temperature. The τ_c value for solid dispersions containing 20% PVP was 2–3 times longer than that for solid dispersions containing 20% HPMC at 50°C , indicating that the molecular mobility of FLF in solid dispersions containing 20% PVP was lower than that in solid dispersions containing 20% HPMC. The amount of amorphous FLF remaining in the solid dispersions stored at 60°C was successfully estimated by analyzing the solid echo signals of FLF fluorine atoms, and it was possible to follow the overall crystallization of amorphous FLF in the solid dispersions. The solid dispersion containing 20% PVP was more stable than that containing 20% HPMC. The difference in stability between solid dispersions containing PVP and HPMC is considered due to the difference in molecular mobility as determined by τ_c . The molecular mobility determined by ^{19}F -NMR seems to be a useful measure for assessing the stability of drugs containing fluorine atoms in amorphous solid dispersions.

Key words ^{19}F -NMR; molecular mobility; stability; crystallization; solid dispersion

Amorphous solid dispersions are used for improving the dissolution rate and solubility of poorly soluble drugs. However, drugs in amorphous form are generally less stable than crystalline drugs because of their higher energy state and higher molecular mobility. It is well known that polymeric excipients can reduce the crystallization rate of many amorphous drugs.^{1–12} This stabilization by poly(vinylpyrrolidone) (PVP) is partly attributable to its ability to decrease molecular mobility, as indicated by increases in the glass transition temperature (T_g).⁹ Therefore, it is of great interest to estimate the molecular mobility of drugs in solid dispersions. Although ^{13}C -NMR relaxation measurements are useful for assessing the molecular mobility of drugs in solid dispersions,¹³ the low sensitivity of ^{13}C because of its low natural abundance is a drawback of ^{13}C -NMR. In contrast to ^{13}C , ^{19}F has very favorable sensitivity in NMR experiments, since it is present in 100% natural abundance, is second only to the proton in its resonance frequency (except ^3H) and has a spin quantum number of 1/2. The receptivity for ^{19}F is 83% of that for ^1H and 4700 times of that for ^{13}C .¹⁴ Many drugs containing fluorine atoms are listed in The Japanese Pharmacopoeia. In contrast, almost all pharmaceutical excipients do not contain fluorine atoms. ^{19}F -NMR may therefore have an advantage over ^{13}C -NMR or ^1H -NMR for selectivity and sensitivity when assessing the molecular mobility of drugs containing fluorine atoms in pharmaceutical dosage forms such as solid dispersions.

The orientations and molecular mobility of flufenamic acid (FLF)¹⁵ and ^{19}F -labeled α -tocopherol¹⁶ in a lipid bilayer were studied using ^{19}F -NMR. Structures and molecular mobility of ^{19}F -labeled peptides and proteins in biological membranes were also investigated.^{17–20} To the authors' knowledge, application of ^{19}F -NMR to studies of drug molecular mobility in solid dispersions has not been reported.

This paper describes the feasibility of ^{19}F -NMR for assessing the molecular mobility of FLF in PVP or hydroxypropylmethylcellulose (HPMC) solid dispersions, and discusses the effect of polymer excipients on the crystallization tendency of FLF in solid dispersions in terms of differences in molecular mobility.

Experimental

Materials FLF (Fig. 1) was purchased from Wako Pure Chemical Industry (Osaka), and PVP and HPMC were from Sigma (St. Louis, MO, U.S.A.). FLF solid dispersions with PVP or HPMC were prepared by melting and cooling of mixtures of FLF with PVP or HPMC. The solid dispersions obtained were confirmed to be amorphous from microscopic observation under polarized light.

Nuclear Magnetic Relaxation Measurements ^{19}F -NMR measurements were carried out using a model JNM-MU25 pulsed NMR spectrometer (JEOL DATUM, Tokyo) operating at a resonance frequency of 25 MHz. Time profiles of spin-spin relaxation of the ^{19}F atoms of FLF were measured using the "solid echo" pulse sequence to overcome the dead time of the instrument. Spin-lattice relaxation time in the laboratory frame (T_1) was measured using the inversion recovery pulse sequence. Spin-lattice relaxation time in the rotating frame ($T_{1\rho}$) was measured at spin locking intensity of 10 G.

DSC Measurements T_g of FLF-PVP and FLF-HPMC solid dispersions was measured by DSC using a model 2920 differential scanning calorimeter and a refrigerator cooling system (TA Instruments, Newcastle, DE, U.S.A.). Approximately 5 mg of each solid dispersions was put into an aluminum sample pan and then sealed hermetically. T_g was measured at a heating rate of $20^\circ\text{C}/\text{min}$. Temperature calibration of the instrument was carried out using indium.

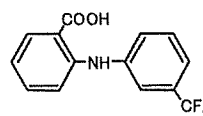


Fig. 1. Structure of FLF

* To whom correspondence should be addressed. e-mail: aso@nihs.go.jp

Results and Discussion

Molecular Mobility of FLF as Measured by ^{19}F -NMR Spin-Lattice Relaxation Time T_1 and $T_{1\rho}$ of fluorine atoms of FLF in PVP and HPMC solid dispersions were measured using a pulsed NMR spectrometer in the temperature range from -20 to 150°C . T_1 is sensitive to the molecular motion on the time scale of the resonance frequency (MHz order). On the other hand, $T_{1\rho}$ is sensitive to the molecular motion with a frequency equivalent to the intensity of spin locking field (typically mid kHz order).²¹⁾ The temperature dependence of T_1 and $T_{1\rho}$ exhibits minimum at a specific temperature at which the molecules of interest have molecular motion with MHz time scale or mid kHz time scale predominantly. The resonance frequency of 25 MHz, lower than that of a conventional high resolution NMR spectrometer, was used to observe T_1 minimum in the temperature range studied. Figure 2 shows the temperature dependence of T_1 and $T_{1\rho}$ of FLF fluorine atoms in PVP and HPMC solid dispersions. For FLF-PVP solid dispersions (7:3), the minimum of T_1 or $T_{1\rho}$ was observed at about 90°C and 60°C , respectively (Fig. 2A). When the PVP content decreased to 20% (w/w), T_1 and $T_{1\rho}$ of FLF at temperatures above 70°C could not be determined due to rapid crystallization. Similar temperature dependence of T_1 or $T_{1\rho}$ was observed for the FLF-HPMC solid dispersions (Fig. 2B). The temperature difference between T_1 and $T_{1\rho}$ minimum is considered to be due to the difference in the time scale of molecular motion reflected on T_1 (MHz order) and $T_{1\rho}$ (mid kHz order). Since the molecular motion on MHz time scale becomes predominant at higher temperature than molecular motion on mid kHz time scale, T_1 minimum is observed at higher tempera-

ture than $T_{1\rho}$ minimum.

We made following assumptions in order to estimate the molecular mobility of FLF from T_1 and $T_{1\rho}$ of FLF fluorine atoms: first, we assumed that FLF fluorine atoms in the solid dispersions relaxes mainly *via* dipolar interaction, and that the contribution of the spin-rotation interaction mechanism²¹⁾ is negligible. While relaxation *via* the spin-rotation interaction mechanism has been reported for liquid sample,²²⁻²⁴⁾ complete domination of dipolar interactions has been reported for fluorine atoms for polycrystalline van der Waals molecular solid.²⁵⁾ We also made an assumption that the contribution of the cross-relaxation between fluorine and proton atoms can be considered small. It is known that relaxation is not intrinsically single-exponential when cross-relaxation between fluorine and proton atoms takes place.¹⁴⁾ However, we assumed small contribution of the cross-relaxation, because the relaxation of FLF fluorine atoms in the solid dispersions was exponential within experimental uncertainty. In studies of molecular motions, a large number of models describing molecular motions have been proposed for calculation of the spectrum density function.²⁶⁾ We used a simple model that the molecular motion reflected on T_1 or $T_{1\rho}$ is represented by single correlation time for the purpose of comparing the mobility of FLF in the PVP and HPMC solid dispersions. According to the above assumptions, T_1 and $T_{1\rho}$ are described by Eqs. 1 and 2.²¹⁾

$$\frac{1}{T_1} = \frac{6}{20} \frac{\gamma^4 \hbar^2}{r^6} \left\{ \frac{\tau_c}{1 + \omega_0^2 \tau_c^2} + \frac{4\tau_c}{1 + 4\omega_0^2 \tau_c^2} \right\} \quad (1)$$

$$\frac{1}{T_{1\rho}} = \frac{3}{20} \frac{\gamma^4 \hbar^2}{r^6} \left\{ \frac{3\tau_c}{1 + 4\omega_1^2 \tau_c^2} + \frac{5\tau_c}{1 + \omega_0^2 \tau_c^2} + \frac{2\tau_c}{1 + 4\omega_0^2 \tau_c^2} \right\} \quad (2)$$

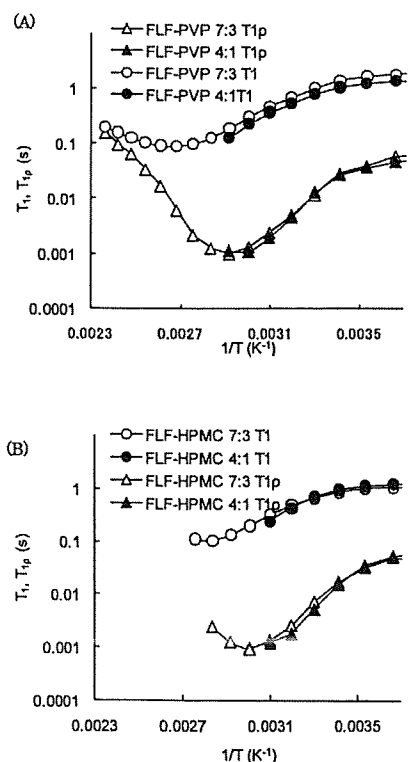


Fig. 2. Temperature Dependence of T_1 and $T_{1\rho}$ of FLF Fluorine Atoms in PVP (A) and HPMC (B) Solid Dispersions

where τ_c is the correlation time that characterizes molecular reorientations, and ω_0 and ω_1 are the resonance frequencies of fluorine atoms in the static magnetic field and spin locking field, respectively. γ , r and \hbar are the gyromagnetic ratio of fluorine, the distance of neighboring fluorine atoms, and the Plank constant divided by 2π , respectively. Equations 1 and 2 infer that T_1 and $T_{1\rho}$ become minimal when $\omega_0 \tau_c$ is approximately 0.62²⁷⁾ and $\omega_1 \tau_c$ is approximately 0.52,²¹⁾ respectively. When the minimum of T_1 or $T_{1\rho}$ is observed, we can calculate the unknown value, r , in Eqs. 1 and 2. If r is known, the τ_c value can be calculated from the observed T_1 or $T_{1\rho}$ value, assuming that r does not change with temperature.

The values of r calculated from the T_1 and $T_{1\rho}$ minimum observed for the FLF-PVP solid dispersion (7:3) were 2.3 and 2.4 Å, respectively, and similar r values were obtained for the FLF-HPMC solid dispersion (7:3). These values are comparable to the reported value (2.174 Å) for 3-(trifluoromethyl)phenanthrene,²⁵⁾ indicating that dipole interaction between neighboring fluorine atoms can be considered the predominant relaxation mechanism of FLF fluorine atoms in the solid dispersions. The difference between the r values obtained in this work and the reported value suggests that the possibility of the spin-rotation interaction mechanism and/or dipole interaction between fluorine and proton atoms cannot be excluded as a relaxation mechanism of FLF fluorine atoms.

Figure 3 shows the temperature dependence of τ_c calculated from T_1 and $T_{1\rho}$ for FLF fluorine atoms in the solid dis-

persions. The τ_c of FLF fluorine atoms in PVP solid dispersions calculated from $T_{1\rho}$ was 8.2 μs at 50 $^\circ\text{C}$, which was about 3 times larger than that in HPMC solid dispersions (2.6 μs), indicating that the molecular mobility of FLF was lowered more strongly by PVP than by HPMC.

The τ_c values calculated using T_1 values differ from those calculated from $T_{1\rho}$ values. The slope of temperature dependence of τ_c changed around T_g . These findings suggest that the assumption that the molecular motion reflected on T_1 and $T_{1\rho}$ is represented by a single τ_c may be too simple to describe the molecular motion of FLF in the solid dispersions at temperatures studied, and that two or more molecular motions, such as rotation of trifluoromethyl group and motions with larger scales than rotation of trifluoromethyl group, may be reflected on T_1 and $T_{1\rho}$. Further studies including $^1\text{H-NMR}$ relaxation measurement and dielectric relaxation measurements will be needed to identify the detailed molecular motion of FLF in the solid dispersions.

Correlation between Crystallization Tendency and Molecular Mobility of FLF in Solid Dispersions Crystallization proceeds *via* formation of crystal nuclei and crystal growth. As a measure of the crystallization tendency of amorphous FLF in solid dispersions, the overall crystallization rate of amorphous FLF in the solid dispersions was estimated from the time profiles amorphous FLF remaining in the solid dispersions instead of measuring the nucleation rate and growth rate. Amorphous FLF remaining in the solid dispersions was estimated by analyzing solid echo signals of FLF fluorine atoms. Figure 4 shows the solid echo signal of

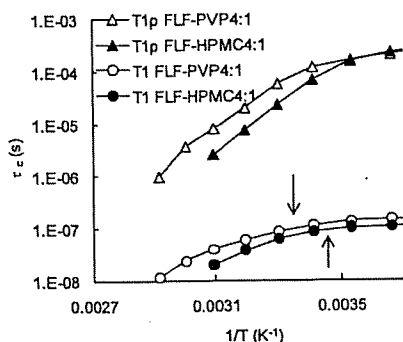


Fig. 3. Temperature Dependence of τ_c of FLF Fluorine Atoms in PVP and HPMC Solid Dispersions

Arrows in the figure represent T_g .

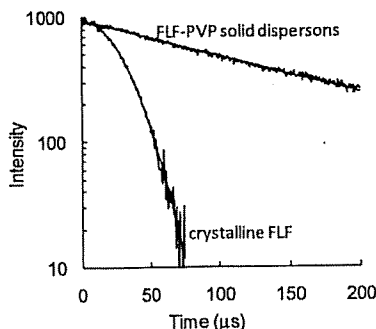


Fig. 4. Typical Solid Echo Signal of Fluorine Atoms of FLF in the Freshly Prepared Solid Dispersion Containing 20% (w/w) PVP and That of Fluorine Atoms of Crystalline FLF

fluorine atoms of FLF in solid dispersions containing 20% (w/w) PVP and that of fluorine atoms of crystalline FLF. The signal for the solid dispersions was describable by the Lorentzian relaxation equation (Eq. 3), and its relaxation time (T_{2L}) was approximately 140 μs . Crystalline FLF exhibited Gaussian relaxation signals (Eq. 4), and its relaxation time (T_{2G}) was approximately 30 μs . These results indicate that amorphous FLF in solid dispersions is considered to exhibit Lorentzian relaxation signals.

$$I=I_0 \exp(-t/T_{2L}) \quad (3)$$

$$I=I_0 \exp(-t^2/(2T_{2G}^2)) \quad (4)$$

where I_0 and I represent the signal intensities at time 0 and t , respectively. Figure 5 shows solid echo signals for the fluorine atoms of FLF in the solid dispersions stored at 60 $^\circ\text{C}$. Samples stored at 60 $^\circ\text{C}$ exhibited biphasic decay signals, and signals were describable by summation of the Gaussian (solid line) and Lorentzian (dashed line) equations (Eq. 5).

$$I=I_0\{P_L \exp(-t/T_{2L})+P_G \exp(-t^2/2T_{2G}^2)\} \quad (5)$$

where P_L and P_G are the ratio of fluorine atoms exhibiting Lorentzian and Gaussian relaxation process, respectively, and $P_L+P_G=1$. Assuming that the T_{2L} and T_{2G} values are 140 and 30 μs , respectively, P_L values of FLF in the solid dispersions were estimated by curve fitting. P_L values of the solid dispersions decreased with increasing storage time, indicating that crystallization of amorphous FLF in solid dispersions takes place during storage at 60 $^\circ\text{C}$. To certify the reliability of the P_L values obtained by $^{19}\text{F-NMR}$ measurements, change in the heat capacity at T_g ($\Delta C_p(T_g)$) was determined for the solid dispersions stored at 60 $^\circ\text{C}$ for various periods as a measure of amorphous FLF remaining, and was compared with the value of P_L . As shown in Fig. 6, the P_L value was proportional to the $\Delta C_p(T_g)$ value, and was considered to be a useful measure of amorphous FLF remaining in the solid dispersions.

Figure 7 shows the time profiles of the P_L values for FLF solid dispersions containing 20% (w/w) PVP or HPMC at 60 $^\circ\text{C}$. The decrease in the ratio of Lorentzian fluorine atoms was faster for HPMC solid dispersions than for PVP solid dispersions, indicating that the overall crystallization rate of FLF in HPMC solid dispersions is larger than that in PVP solid dispersions. The overall crystallization rate depends on both molecular mobility (the rate of diffusion across the interface between crystalline and amorphous phase) and ther-

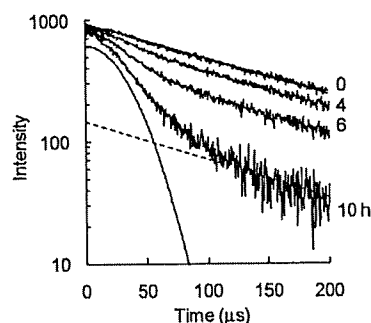


Fig. 5. Typical Solid Echo Signals of Fluorine Atoms of FLF in the Solid Dispersions Containing 20% (w/w) PVP Stored at 60 $^\circ\text{C}$

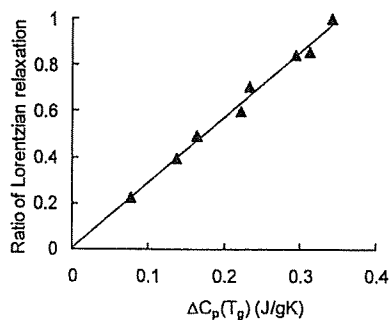


Fig. 6. The Ratio of FLF Fluorine Atoms Exhibiting Lorentzian Relaxation as a Function of Changes in the Heat Capacity at T_g

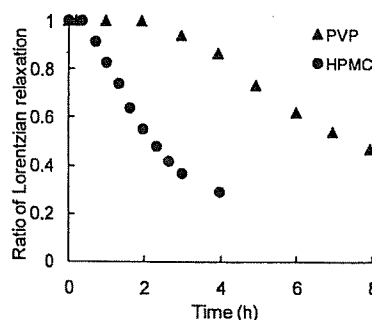


Fig. 7. Time Profiles of the Ratio of FLF Fluorine Atoms Exhibiting Lorentzian Relaxation in PVP and HPMC Solid Dispersions Stored at 60 °C

modynamic factors, such as free energy difference between crystalline and amorphous form.^{2,3,10} Differences in the overall crystallization rate of amorphous FLF are consistent with those in the molecular mobility (Fig. 3), suggesting that the molecular mobility as determined by the ^{19}F -NMR spin-lattice relaxation times may be one of the factors determining crystallization rate, and useful as a measure of the physical stability of FLF in solid dispersions. The T_g values of the solid dispersions containing 20% PVP and 20% HPMC were 23 °C and 15 °C, respectively, indicating that molecular mobility reflected on T_g is higher for the solid dispersion containing HPMC than for that containing PVP. The T_g data seem to support the speculation obtained from NMR data. However, the scale of molecular mobility reflected on T_g is considered to be larger than that reflected on τ_c . Further studies should be conducted to elucidate the quantitative correlation between the physical stability of amorphous FLF and the molecular mobility determined by ^{19}F -NMR.

In conclusion, ^{19}F -NMR is useful for elucidating the molecular mobility of drugs containing fluorine atoms in amorphous solid dispersions. τ_c values of FLF fluorine atoms were calculated from the ^{19}F -NMR spin-lattice relaxation data. The τ_c value for solid dispersions containing 20% PVP

was 2–3 times longer than that for solid dispersions containing 20% HPMC at 50 °C. Molecular mobility of FLF in the solid dispersions containing 20% PVP was lower than in those containing 20% HPMC, and this was consistent with the fact that the overall crystallization rate of amorphous FLF in the solid dispersion containing PVP was smaller than in that containing HPMC. The molecular mobility determined by ^{19}F -NMR seems to be useful as a measure of the physical stability of an amorphous drug in solid dispersions.

Acknowledgements Part of this work was supported by a Grant-in-aid for Research on Publicly Essential Drugs and Medical Devices from The Japan Health Sciences Foundation.

References

- 1) Yoshioka M., Hancock B. C., Zografi G., *J. Pharm. Sci.*, **84**, 983–986 (1995).
- 2) Matsumoto T., Zografi G., *Pharm. Res.*, **16**, 1722–1728 (1999).
- 3) Crowley K. J., Zografi G., *Pharm. Res.*, **20**, 1417–1422 (2003).
- 4) Shamblyn S. L., Huang E. Y., Zografi G., *J. Therm. Anal.*, **47**, 1567–1579 (1996).
- 5) Shamblyn S. L., Zografi G., *Pharm. Res.*, **16**, 1119–1124 (1999).
- 6) Zeng X. M., Martin G. P., Marriott C., *Int. J. Pharm.*, **218**, 63–73 (2001).
- 7) Miyazaki T., Yoshioka S., Aso Y., Kojima S., *J. Pharm. Sci.*, **93**, 2710–2717 (2004).
- 8) Khougaz K., Clas S., *J. Pharm. Sci.*, **89**, 1325–1334 (2000).
- 9) Berggren J., Alderborn G., *Eur. J. Pharm. Sci.*, **21**, 209–215 (2004).
- 10) Aso Y., Yoshioka S., Kojima S., *J. Pharm. Sci.*, **93**, 384–391 (2004).
- 11) Miyazaki T., Yoshioka S., Aso Y., *Chem. Pharm. Bull.*, **54**, 1207–1210 (2006).
- 12) Konno H., Taylor L. S., *J. Pharm. Sci.*, **95**, 2692–2705 (2006).
- 13) Aso Y., Yoshioka S., *J. Pharm. Sci.*, **95**, 318–325 (2006).
- 14) Harris R. K., Monti G. A., Holstein P., "Solid State NMR of Polymers," Chap. 6, ed. by Ando I., Asakura T., Elsevier, Amsterdam, 1998, pp. 351–414.
- 15) Grage S. L., Ulrich A. S., *J. Magn. Reson.*, **146**, 81–88 (2000).
- 16) Urano S., Matsuo M., Sakanaka T., Uemura I., Koyama M., Kumadaki I., Fukuzawa K., *Arch. Biochem. Biophys.*, **303**, 10–14 (1993).
- 17) Afonin S., Glaser R. W., Berdichevskaja M., Wadhvani P., Gührs K. H., Möllmann U., Perner A., Ulrich A. S., *ChemBioChem*, **4**, 1151–1163 (2003).
- 18) Salgado J., Grage S. L., Kondejewski L. H., Hodges R. S., McElhane R. N., Ulrich A. S., *J. Biomol. NMR*, **21**, 191–208 (2001).
- 19) Williams S. P., Haggie P. M., Brindle K. M., *Biophys. J.*, **72**, 490–498 (1997).
- 20) Quint P., Ayala I., Busby S. A., Chalmers M. J., Griffin P. R., Rocca J., Nick H. S., Silverman D. N., *Biochemistry*, **45**, 8209–8215 (2006).
- 21) Farrar T. C., Brcker E. D., "Pulse and Fourier Transform NMR," Academic Press, New York and London, 1971.
- 22) Namgoong H., Lee J. W., *Bull. Korean Chem. Soc.*, **14**, 91–95 (1993).
- 23) Huang S.-G., Rogers M. T., *J. Chem. Phys.*, **68**, 5601–5606 (1978).
- 24) Gutowsky H. S., Lawrence I. J., Shimomura K., *Phys. Rev. Lett.*, **6**, 349–351 (1961).
- 25) Beckmann P. A., Rosenberg J., Nordstrom K., Mallory C. W., Mallory F. B., *J. Phys. Chem. A*, **110**, 3947–3953 (2006).
- 26) Horii F., "Solid State NMR of Polymers," Chap. 3, ed. by Ando I., Asakura T., Elsevier, Amsterdam, 1998, pp. 51–82.
- 27) Ruan R. R., Chen P. L., "Water in Foods and Biological Materials," Chap. 7, Technomic Publishing Co., Lancaster Basel, 1998, pp. 253–278.

Forum Minireview

New Aspects for the Treatment of Cardiac Diseases Based on the Diversity of Functional Controls on Cardiac Muscles: Diversity in the Excitation–Contraction Mechanisms of the Heart

Hikaru Tanaka^{1,*}, Iyuki Namekata¹, Hideaki Nouchi¹, Koki Shigenobu¹, Toru Kawanishi², and Akira Takahara¹

¹Department of Pharmacology, Toho University Faculty of Pharmaceutical Sciences, Chiba 274-8510, Japan

²Division of Drugs, National Institute of Health Science, Tokyo 158-8501, Japan

Received October 16, 2008; Accepted November 5, 2008

Abstract. The waveform of the myocardial action potential (AP) triggering contraction differs among the species, developmental stage, and pathological state. The species difference in heart rate, which inversely correlates with body size, originates in the ion-channel mechanisms responsible for diastolic depolarization of the sinoatrial node. In some cases, such as the chronically AV-blocked dog and 11- to 13-day chick embryo, the repolarization reserve is decreased making the heart useful for drug evaluation. The degree of dependence of contraction on sarcoplasmic reticulum (SR) function increases during development. The large SR dependence and short AP of the adult mouse and rat support their rapid contraction under high heart rate. The function of the Na⁺/Ca²⁺ exchanger is affected by AP waveform and ion concentrations; its major role is Ca²⁺ extrusion, but under pathological conditions such as ischemia-reperfusion, it allows Ca²⁺ influx and leads to myocardial injury, including loss of mitochondrial function. The role of mitochondria in ATP supply is less in the fetus where glycolysis plays a greater role. The pharmacological properties of the myocardium are affected by all of these factors and also by autonomic innervation and the hormonal status. Such comprehensive understanding is indispensable for the development of novel therapeutic strategies.

Keywords: heart, action potential, contraction, calcium ion, autonomic nervous system, cardiac disease

Introduction

The action potential and the Ca²⁺ transient are the common mechanisms triggering myocardial contraction, but the precise mechanisms for the generation of the action potential and Ca²⁺ handling as well as their neurohormonal regulation differs among the species, developmental stage, and pathological state. In general, the hearts of smaller animals have higher beating rates, which could be ascribed to a difference in the pacemaker depolarization mechanisms of the sinoatrial node. The time course of repolarization and Ca²⁺ transient is faster in the myocardium of smaller animals, which can be

ascribed to ion-channel and Ca²⁺-handling mechanisms. Such difference in the basic excitation–contraction mechanisms underlies the difference in pharmacological properties of the myocardium. In general, difference among species is small in the immature myocardium and become prominent towards adulthood. The pharmacological properties of the myocardium are also affected by the metabolic background and also by the presence of non-myocardial cells in the myocardium such as neurons and endocardial endothelial cells. Here we will overview the factors underlying the diversity in myocardial excitation–contraction mechanisms. For details, refer to recent reviews in each field.

Pacemaker mechanisms

Cardiac pacemaking is the result of multiple ionic

*Corresponding author. htanaka@phar.toho-u.ac.jp
Published online in J-STAGE on March 7, 2009 (in advance)
doi: 10.1254/jphs.08R22FM

mechanisms in the sinoatrial node cell (1, 2). Ion channels including the L-type calcium current (I_{CaL}), sustained inward current (I_{st}), hyperpolarization-activated inward current (I_h or I_f), T-type calcium current (I_{CaT}), and sodium calcium exchanger current (I_{NCX}) have been reported to be involved in the depolarization of the sinoatrial node action potential. The contribution of each component appears to vary among animal species. The action potential upstroke is caused by I_{CaL} , whose molecular identity was reported to include two different pore-forming subunits, Cav1.2 and Cav1.3. Most of the I_{CaL} flows through Cav1.2 in the mouse sinoatrial node while that in the porcine sinoatrial node flows exclusively through Cav1.3 (2). I_{CaT} appears to contribute to the pacemaker (phase 4) depolarization but only in smaller animals (2). Results from voltage clamp experiments as well as analysis with the selective I_{CaT} blocker $R(-)$ -efonidipine (3) revealed that the I_{CaT} density in sinoatrial node cells is higher in smaller animals such as the mouse and low in larger animals such as the rabbit and pig. There is no report on the species difference of I_h and I_{st} . I_h may rather be involved in the regional variation in the maximum diastolic potential within the sinoatrial node region: the density is higher in the peripheral region of the sinoatrial node, which may function to protect the pacemaking activity at the central region from the hyperpolarizing influence of the surrounding atrial cells (1).

The rate of repolarization is determined by the density and type of potassium currents present in the sinoatrial node cells (2). The delayed rectifier potassium current I_K consists of two components, the rapidly activating I_{Kr} and the slowly activating I_{Ks} . Selective blockade of I_{Kr} by E-4031 inhibits spontaneous activity of the rabbit, guinea-pig and mouse sinoatrial node cells, and blockade of I_{Ks} by chromanol 293B inhibits those in porcine and guinea-pig sinoatrial node cells. These results suggest that the sinoatrial node automaticity is driven by I_{Kr} in smaller animals with high sinus rate and by I_{Ks} in larger animals with slower sinus rate. Some researchers postulate that pacemaking is also controlled by an intracellular clock; Ca^{2+} released from the sarcoplasmic reticulum during the diastolic period is pumped out of the cell through the forward-mode Na^+/Ca^{2+} exchanger that generates an inward current and may contribute to pacemaker depolarization (4). However, others reported that the automaticity of the sinoatrial node cells was not abolished by ryanodine, which interferes with sarcoplasmic reticulum function (5). Such discrepancy may reflect the regional variations in pacemaker mechanisms; the contribution of the intracellular clock may be larger in the peripheral region of the sinoatrial node (6). The myocardium present in the pulmonary vein, which is attracting attention as the source of ectopic auto-

maticity responsible for the generation and maintenance of atrial fibrillation, was shown to have action potential properties different from those of the atrium (7). It shows spontaneous and ouabain-induced automaticity, which can be inhibited by either ryanodine or the Na^+/Ca^{2+} exchanger blockade. Thus, acceleration of pacemaker depolarization by the intracellular clock may be prominent in certain regions of the myocardium and/or under pathological conditions.

Action potential properties in the working myocardium

Concerning the action potential of the working myocardium, diversity is observed in the repolarization phase rather than in the depolarization phase (8). The rapid upstroke of the action potential is caused by a large I_{Na} current density that guarantees propagation of the action potential through the myocardium (9). In the adult mouse ventricular myocardium, the upstroke velocity is more than twofold higher than those observed in most other working myocardia. This might be a mechanism to compensate for the extremely short action potential duration in the adult mouse ventricle; shorter action potential duration means less electrotonic depolarizing support from behind at the activation wave front. A large diversity exists in the rate of the repolarization and the ionic currents involved among animal species and the developmental stage (ref. 8 and Fig. 1). The adult mouse ventricular myocardium has an action potential with extremely short duration at depolarized potentials of only a few ms and a late slowly repolarizing phase. Voltage clamp studies showed that the I_{Ca} density of the mouse and rat myocardium is not less than that of other species such as the guinea pig and rabbit, which has an action potential lasting as long as 200 ms. The repolarizing potassium current of the mouse and rat ventricle is the transient outward current (I_{to}), which activates much faster than I_K , the major repolarizing current of ventricular myocardia in many other animals. Thus, the diversity in repolarizing potassium currents appears to be the major cause of species difference in myocardial repolarization.

The potassium currents responsible for repolarization are influenced by the endocrine hormones and are reduced under pathological conditions and in the immature myocardium. A cardiac ion channel responsible for repolarization is known to be affected by sex hormones (10). This can at least partly explain the observed gender difference in susceptibility to the arrhythmogenic effects of QT-prolonging drugs. The hearts of the chronic AV block dog were shown to undergo structural remodeling including myocardial hypertrophy and in-

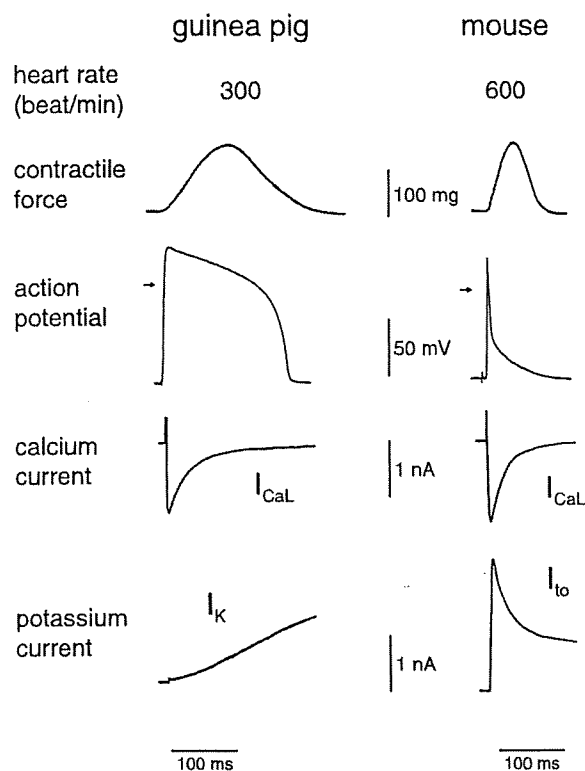


Fig. 1. Species difference in myocardial excitation-contraction properties. Typical records for the contractile force, action potential, and membrane currents of isolated myocardial tissue and cells were compared between the guinea pig and mouse.

crease in collagen fibers (11). This was accompanied by decreased expression level of potassium channels, resulting in increased action potential duration in the AV-blocked dog myocardium (12). It was also shown to have an increased sensitivity to the action potential prolonging and/or arrhythmogenic effect of drugs with potassium channel-blocking activity. Reduced repolarizing currents have been reported in immature myocardia from many animal species. In case of the guinea

pig ventricle, the densities of I_{Ca} and I_K are both decreased in the fetus compared to those in the adult (13). The fetal ventricle has an action potential with longer duration and a higher sensitivity to the prolonging effect of pharmacological agents (14). Ventricular myocardium from the 11- to 13-day chick embryo also has an increased sensitivity to action potential prolonging drugs (15). I_K blockade with E-4031 prolongs the action potential duration at this age and induces early afterdepolarization. Terfenadine, which is known for its lack of action potential-prolonging activity on isolated myocardial tissue preparations despite its QT-prolonging and arrhythmogenic activity in vivo, was shown to produce action potential prolongation in the 11- to 13-day chick embryo ventricle. Thus, myocardia from certain pathological models and from immature animals appear to have decreased repolarization reserve and may be a useful model for the investigation of arrhythmogenic mechanisms and a sensitive assay system for the action potential prolonging activity of drugs.

Ca²⁺ handling

Ventricular myocytes from the adult mammalian heart have a well-developed T-tubular system throughout the cell. During the action potential plateau, Ca²⁺ influx through the sarcolemma and T-tubules triggers Ca²⁺ release from ryanodine receptors located on the adjacent sarcoplasmic reticulum membrane. These results in a higher Ca²⁺ concentration at the Z-band region of the ventricular myocyte only for several milliseconds during the early phase of contraction, and at about 10 ms after the onset of the action potential, Ca²⁺ concentration is uniform throughout the whole cytoplasm (16). Variations exist in the relative contribution of the transsarcolemmal Ca²⁺ influx and Ca²⁺ release from the sarcoplasmic reticulum (ref. 8 and Fig. 2). The potency order for the negative inotropic effect of nifedipine, which reflects dependence on transsarcolemmal Ca²⁺ influx, was mouse < rat < guinea pig. This correlated with the species

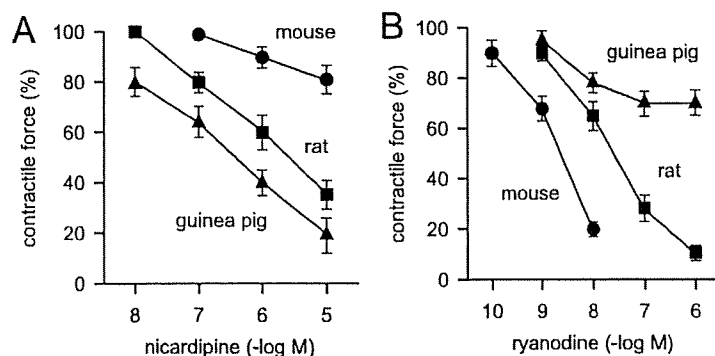


Fig. 2. Species difference in the calcium source for contraction. Negative inotropic effects of nifedipine (A), an inhibitor of transsarcolemmal Ca²⁺ influx, and ryanodine (B), an inhibitor of Ca²⁺ release from the sarcoplasmic reticulum, were compared between isolated ventricular preparations from the mouse (circles), rat (squares), and guinea pig (triangles).

difference in action potential duration. On the other hand, the potency order for the negative inotropic effects of ryanodine and cyclopiazonic acid, which reflects dependence on Ca^{2+} release from the sarcoplasmic reticulum, was mouse > rat > guinea pig. This was the same as the order of the myocardial relaxation rate. Comparative studies with various mammals revealed that hearts of smaller weight have higher resting sinus rate and higher sarcoplasmic reticulum Ca^{2+} ATPase activity. Hearts with higher beating rate require faster contraction and relaxation for sufficient refilling before the next heartbeat, which can be accomplished by increasing sarcoplasmic reticulum function. Such species difference in excitation-contraction mechanism is less prominent in immature myocardia. In the fetal myocardia, the size of the cardiomyocytes is small and the sarcoplasmic reticulum and T-tubular system are scarcely developed (17). This results in a higher dependence of contraction on transsarcolemmal Ca^{2+} influx.

In contrast to the adult ventricular myocardia where a large species difference was observed, the atrial myocardia of the mouse, rat, and guinea pig were shown to have similar high inotropic sensitivity to ryanodine, which could be explained by the atrial excitation-contraction coupling mechanisms (18). In atrial cardiomyocytes that lack a T-tubular system, transsarcolemmal Ca^{2+} influx triggers Ca^{2+} release only at the subsarcolemmal sarcoplasmic reticulum. This Ca^{2+} triggers Ca^{2+} release from the neighboring sarcoplasmic reticulum and a wave of Ca^{2+} -induced Ca^{2+} release propagates towards the cell interior. Ca^{2+} waves were more sensitive to ryanodine and cyclopiazonic acid than Ca^{2+} transients evoked by action potentials. Involvement of Ca^{2+} waves in normal atrial excitation-contraction coupling can explain the high sensitivity of atrial contraction to these agents regardless of the animal species.

Sympathetic regulation

The sympathetic nervous system is the major accelerator of myocardial function, which increases myocardial contractile force through β -adrenoceptor-mediated activation of adenylate cyclase in most animal species (19). The inotropic sensitivity to the sympathetic neurotransmitter noradrenaline is known to be affected by various factors. It is increased by hyperthyroidism and decreased under diabetic conditions. Sympathetic innervation itself exerts long-term influence on the myocardium including maintenance of its sensitivity to its own neurotransmitter. Sympathetic denervation of the heart results in supersensitivity of the myocardium not only to noradrenaline but also to other transmitters such as acetylcholine (20, 21). The fetal heart is initially

devoid of sympathetic innervation. In the case of the rat, sympathetic innervation occurs at fetal day 17 at the sinoatrial node and from late embryonic period in the ventricle. The development of sympathetic innervation is followed by a tenfold decrease in the chronotropic and inotropic sensitivity of the β -adrenoceptor-mediated mechanisms (22). The time course of the functional development of the sympathetic nervous system as well as the sensitivity to autonomic transmitters are altered in pathological models such as the spontaneously hypertensive rat (23). Disturbance of the normal development of the sympathetic innervation results in alterations in responsiveness to β -adrenergic stimulation and increased susceptibility to arrhythmogenic stimuli (24). Recent studies on the roles of adenylate cyclase isoforms in the myocardium suggest that isoform-specific manipulation of the enzyme may be of value in the treatment of heart failure (25).

α -Adrenoceptors are present in the myocardium and their stimulation results in no or weak positive inotropy through mechanisms different from those of β -adrenoceptor stimulation (19). Sustained positive inotropy is observed in the rabbit, guinea pig, and rat ventricle, but in the guinea pig and rat, a transient decrease in contractile force is observed before the increase. The mouse ventricle shows a sustained negative inotropy in response to α -adrenoceptor stimulation (26) that is accompanied by decreased calcium transient amplitude (27). Electrophysiological and pharmacological analysis revealed that α -adrenoceptor stimulation activates the $\text{Na}^+/\text{Ca}^{2+}$ exchanger and decreases the Ca^{2+} released from the sarcoplasmic reticulum (28). Interestingly, activation of the $\text{Na}^+/\text{Ca}^{2+}$ exchanger following α -adrenoceptor stimulation was also observed in guinea-pig ventricular myocytes. The extremely short action potential of the mouse ventricular myocyte favors the $\text{Na}^+/\text{Ca}^{2+}$ exchanger to function in the forward (Ca^{2+} extrusion) mode and decrease the Ca^{2+} transient amplitude and contractile force. In fact, in the neonatal mouse ventricle, which has an action potential of longer duration, α -adrenoceptor-mediated inotropy is positive. Similar developmental conversion of inotropy from positive to negative is observed in the mouse ventricle with endothelin I and angiotensin II (29). These results suggest that the inotropic responses of the myocardium to various active substances are largely affected by the basic excitation-contraction properties of the myocardium.

Muscarinic receptor-mediated regulation

In the ventricular myocardium, the parasympathetic neurotransmitter acetylcholine is generally considered to

show no inotropy under basal conditions and negative inotropy after elevation of adenylate cyclase activity by adrenoceptor stimulation (19). In some cases, direct negative inotropy by muscarinic receptor stimulation has been reported in ventricles from the ferret, rat, dog, and hatched chick. The negative inotropy was mediated by hyperpolarization and decrease in action potential duration in the case of the ferret, while inhibition of an intrinsically activated adenylate cyclase activity was the likely mechanism in the case of the hatched chick (30). In mammalian atria, acetylcholine is considered to produce negative inotropy through inhibition of adenylate cyclase and activation of the G-protein coupled potassium current $I_{K_{ACH}}$. However, there are cases in which acetylcholine induces positive inotropy. In the chick embryonic atria, acetylcholine induces positive inotropy through stimulation of M_1 receptors and activation of phospholipase C. Muscarinic receptors are known to be present not only in cardiomyocytes but also in other cell types in the myocardium. In mouse atria, a biphasic inotropic response to acetylcholine was observed: a transient negative inotropy was followed by positive inotropy that were both inhibited with atropine (31). The positive inotropy in this case was revealed to be mediated by prostaglandins released from the endocardial endothelium (32). In other cases, muscarinic agonist-induced positive inotropy was mediated by noradrenaline released from sympathetic nerve terminals. There seems to be a large variation in the polarity and mechanism for the acetylcholine-induced inotropy, which reflects both the intrinsic properties of the cardiomyocyte and the influence of other cell types in the myocardium. Whether these mechanisms are related to the pathophysiology of the heart and the effects of therapeutic agents awaits further investigation.

Effects of ischemia

The adult myocardium has a high mitochondrial content and capacity for oxidative metabolism to produce ATP. Ischemia or hypoxia, resulting from a disruption or reduction of the coronary blood flow in vivo or its simulation in experimental systems, results in myocardial injury including Ca^{2+} overload, decreased resting membrane potential and action potential duration, loss of mitochondrial function and decreased ATP content, and marked reduction of the contractile force. Such damage is only partially recovered even if the coronary perfusion is recovered. Many agents have been reported to show protective effects against myocardial ischemia-reperfusion damage (33). In most cases, the protection appeared to be accompanied by drug-induced reduction of myocardial performance. Some agents such as Cl^-

channel blockers (34) and Na^+/Ca^{2+} -exchanger inhibitors (35) showed protection against myocardial ischemia-reperfusion injury with no evidence of cardioppression. Evidence available at present suggests that preservation of mitochondrial function is involved in the protective effect of these agents (36). Various ion channels and transporters are present on the mitochondrial membrane and their modulation has been reported to affect mitochondrial function (37). Agents that open mitochondrial K^+ channels prevents mitochondrial Ca^{2+} overload and preserves its function through partial depolarization of the mitochondrial inner membrane.

There seem to be some variations in the susceptibility to injury during ischemia and reperfusion. The hypertrophied myocardium exposed to sustained pressure- or volume-overload is known to have increased susceptibility, which may be the result of altered metabolic properties (38). Myocardial long-chain fatty acid oxidation and coupling between glycolysis and glucose oxidation are lower than normal, resulting in enhanced H^+ production in hypertrophied myocardium. Some researchers postulate that agents that alter myocardial energy metabolism through inhibition of fatty acid oxidation may be beneficial for cardioprotection against ischemic insult. The susceptibility of the myocardium to ischemic insult is also different between mature and immature myocardium. In the adult guinea-pig ventricle, experimental hypoxia results in marked shortening of the action potential duration and complete loss of contractile activity (39). In contrast, both the action potential duration and contractile force were partly maintained in the fetal ventricle. The ATP-sensitive K^+ channel, which is considered to be the primary cause of action potential shortening under hypoxic conditions, was present in similar densities in cardiomyocytes from the adult and fetus. The relative resistance to hypoxia of the fetal myocardium could rather be explained by its high dependence on glycolysis. In general, the developmental conversion of metabolism from anaerobic to aerobic appears to parallel the increase in susceptibility to ischemic insult. Thus, the most effective strategy for cardioprotection against ischemia-reperfusion may vary depending on the metabolic status of the myocardium.

Conclusion

A large diversity exists in the excitation-contraction mechanism of the myocardium that reflects diversity in the ultrastructure of the cardiomyocyte, type and amount of ion channels and various functional proteins expressed, and the metabolic status of the myocardium. These basic properties are influenced by non-cardiac cells present in the myocardium such as neurons and endocardial endo-

thelial cells, and they are altered under pathological conditions. Diversity in the chronotropic and inotropic responses to neuronal and hormonal stimuli and to various pharmacological agents can be partly explained by the underlying excitation-contraction properties. Such comprehensive understanding of the myocardium is indispensable for the extrapolation of experimental findings to the human heart and for the development of novel therapeutic strategies.

Acknowledgments

Some of the studies performed by our group was a part of the project "Research on the molecular mechanisms of appearance of age-related diseases by failure of cell function control system, and their prevention and treatment" by the "Research Center for Aging and Age related Diseases" established in the Toho University Faculty of Pharmaceutical Sciences, and was supported in part by a grant-in-aid for Research on Publicly Essential Drugs and Medical Devices to K.S. and T.K. from the Japan Health Science Foundation.

References

- Boyett MR, Honjo H, Kodama I. The sinoatrial node, a heterogeneous pacemaker structure. *Cardiovasc Res.* 2000;47:658-687.
- Ono K, Iijima T. Ionic and molecular basis of cardiac automaticity in mammalian heart. In: Mizukami Y, Ohtsuka T, editors. *Molecular mechanisms of heart diseases*. Trivandrum: Research SignPost; 2005. p.1-22.
- Tanaka H, Komikado C, Namekata I, Nakamura H, Suzuki M, Tsuneoka Y, et al. Species difference in the contribution of T-type calcium current to cardiac pacemaking as revealed by R(-)-efenidipine. *J Pharmacol Sci.* 2008;107:99-102.
- Maltsev VA, Vinogradova TM, Lakatta EG. The emergence of a general theory of the initiation and strength of the heartbeat. *J Pharmacol Sci.* 2006;100:338-369.
- Honjo H, Inada S, Lancaster MK, Yamamoto M, Niwa R, Jones SA, et al. Sarcoplasmic reticulum Ca²⁺ release is not a dominating factor in sinoatrial node pacemaker activity. *Circ Res.* 2003;92:e41-e44.
- Lancaster MK, Jones SA, Harrison SM, Boyett MR. Intracellular Ca²⁺ and pacemaking within the rabbit sinoatrial node: heterogeneity of role and control. *J Physiol.* 2004;556(Pt 2):481-494.
- Melnyk P, Ehrlich JR, Pourrier M, Villeneuve L, Cha TJ, Nattel S. Comparison of ion channel distribution and expression in cardiomyocytes of canine pulmonary veins versus left atrium. *Cardiovasc Res.* 2005;65:104-116.
- Tanaka H, Shigenobu K. Species difference in myocardial excitation-contraction coupling featuring the mouse. *Curr Topics Pharmacol.* 2003;7:247-256.
- Tanaka H, Sekine T, Nishimaru K, Shigenobu K. Role of sarcoplasmic reticulum in myocardial contraction of neonatal and adult mice. *Comp Biochem Physiol A Mol Integr Physiol.* 1998;120:431-438.
- Kurokawa J, Suzuki T, Furukawa T. New aspects for the treatment of cardiac diseases based on the diversity of functional controls on cardiac muscles: Acute effects of female hormones on cardiac ion channels and cardiac repolarization. *J Pharmacol Sci.* 2009;109:334-340.
- Sugiyama A, Ishida Y, Satoh Y, Aoki S, Hori M, Akie Y, et al. Electrophysiological, anatomical and histological remodeling of the heart to AV block enhances susceptibility to arrhythmogenic effects of QT-prolonging drugs. *Jpn J Pharmacol.* 2002;88:341-350.
- Takahara A, Nakamura H, Nouchi H, Tamura T, Tanaka T, Shimada H, et al. Analysis of arrhythmogenic profile in a canine model of chronic atrioventricular block by comparing in vitro effects of the class III antiarrhythmic drug nifekalant on the ventricular action potential indices between normal heart and atrioventricular block heart. *J Pharmacol Sci.* 2007;103:181-188.
- Kato Y, Masumiya H, Agata N, Tanaka H, Shigenobu K. Developmental changes in action potential and membrane currents in fetal, neonatal and adult guinea-pig ventricular myocytes. *J Mol Cell Cardiol.* 1996;28:1515-1522.
- Agata N, Tanaka H, Shigenobu K. Developmental changes in action potential properties of the guinea pig myocardium. *Acta Physiol Scand.* 1994;149:331.
- Nouchi H, Kiryu N, Tanaka H, Shigenobu K. Developmental changes in the effect of K channel blockers on the chick ventricular action potential. *J Pharmacol Sci.* 2007;103:Suppl I:202P.
- Tanaka H, Sekine T, Kawanishi T, Nakamura R, Shigenobu K. Intracellular [Ca²⁺] gradients and their spatio-temporal relation to Ca²⁺ sparks in rat cardiomyocytes. *J Physiol.* 1998;508:145-152.
- Seki S, Nagashima M, Yamada Y, Tsutsuura M, Kobayashi T, Namiki A, et al. Fetal and postnatal development of Ca²⁺ transients and Ca²⁺ sparks in rat cardiomyocytes. *Cardiovasc Res.* 2003;58:535-548.
- Tanaka H, Masumiya H, Sekine T, Kawanishi T, Hayakawa T, Miyata S, et al. Involvement of Ca²⁺ waves in excitation contraction coupling of rat atrial cardiomyocytes. *Life Sci.* 2001;70:715-726.
- Endoh M. Signal transduction and Ca²⁺ signaling in intact myocardium. *J Pharmacol Sci.* 2006;100:525-537.
- Ishii K, Shigenobu K, Kasuya Y. Postjunctional supersensitivity in young rat heart produced by immunological and chemical sympathectomy. *J Pharmacol Exp Ther.* 1982;220:209-215.
- Ishii K, Ishii N, Shigenobu K, Kasuya Y. Acetylcholine supersensitivity in the rat heart produced by neonatal sympathectomy. *Can J Physiol Pharmacol.* 1985;63:898-899.
- Tanaka H, Shigenobu K. Role of β -adrenoceptor-adenylate cyclase system in the developmental decrease in sensitivity to isoproterenol in fetal and neonatal rat heart. *Br J Pharmacol.* 1990;100:138-142.
- Tanaka H, Kasuya Y, Shigenobu K. Altered responsiveness to autonomic transmitters of hearts from neonatal spontaneously hypertensive rats. *J Cardiovasc Pharmacol.* 1988;12:678-682.
- Ieda M, Fukuda K. New aspects for the treatment of cardiac diseases based on the diversity of functional controls on cardiac muscles: The regulatory mechanisms of cardiac innervation and their critical roles in cardiac performance. *J Pharmacol Sci.* 2009;109:348-353.
- Okumura S, Suzuki S, Ishikawa Y. New aspects for the treatment of cardiac diseases based on the diversity of functional controls on cardiac muscles: Effects of targeted disruption of the type 5

- adenylyl cyclase gene. *J Pharmacol Sci.* 2009;109:354–359.
- 26 Tanaka H, Manita S, Matsuda T, Adachi M, Shigenobu K. Sustained negative inotropism mediated by alpha-adrenoceptors in adult mouse myocardia: developmental conversion from positive response in the neonate. *Br J Pharmacol.* 1995;114:673–677.
- 27 Tanaka H, Namekata I, Takeda K, Shimizu Y, Moriwaki R, Hirayama W, et al. Unique excitation-contraction characteristics of mouse myocardium as revealed by SEA0400, a specific inhibitor of Na⁺-Ca²⁺ exchanger. *Naunyn Schmiedebergs Arch Pharmacol.* 2005;371:526–534.
- 28 Nishimaru K, Tanaka Y, Tanaka H, Shigenobu K. α -Adrenoceptor stimulation-mediated negative inotropism and enhancement of Na⁺-Ca²⁺ exchange in mouse ventricle. *Am J Physiol.* 2001;280:H132–H141.
- 29 Sekine T, Kusano H, Nishimaru K, Tanaka Y, Tanaka H, Shigenobu K. Developmental conversion of inotropism by endothelin I and angiotensin II from positive to negative in mice. *Eur J Pharmacol.* 1999;374:411–415.
- 30 Nouchi H, Kaeriyama S, Muramatsu A, Sato M, Hirose K, Shimizu N, et al. Muscarinic receptor subtypes mediating positive and negative inotropy in the developing chick ventricle. *J Pharmacol Sci.* 2007;103:75–82.
- 31 Nishimaru K, Tanaka Y, Tanaka H, Shigenobu K. Positive and negative inotropic effects of muscarinic receptor stimulation in mouse left atria. *Life Sci.* 2000;66:607–615.
- 32 Tanaka H, Nishimaru K, Kobayashi M, Matsuda T, Tanaka Y, Shigenobu K. Acetylcholine-induced positive inotropism mediated by prostaglandin released from endocardial endothelium in mouse left atrium. *Naunyn Schmiedebergs Arch Pharmacol.* 2001;363:577–582.
- 33 Gover GJ, Sleph PG. Dissociation of cardiodepression from cardioprotection with calcium antagonists: diltiazem protects ischemic rat myocardium with a lower functional cost as compared with verapamil or nifedipine. *J Cardiovasc Pharmacol.* 1989;14:331–340.
- 34 Tanaka H, Matsui S, Kawanishi T, Shigenobu K. Use of chloride blockers: a novel approach for cardioprotection against ischemia-reperfusion damage. *J Pharmacol Exp Ther.* 1996;278:854–861.
- 35 Namekata I, Nakamura H, Tanaka H, Shigenobu K. Cardioprotection without cardiosuppression by SEA0400, a novel inhibitor of Na⁺-Ca²⁺ exchanger, during ischemia-reperfusion injury in guinea-pig myocardium. *Life Sci.* 2005;77:312–324.
- 36 Namekata I, Shimada H, Kawanishi T, Tanaka H, Shigenobu K. Reduction by SEA0400 of myocardial ischemia-induced cytoplasmic and mitochondrial Ca²⁺ overload. *Eur J Pharmacol.* 2006;533:108–115.
- 37 Nishida H, Sato T, Ogura T, Nakaya H. New aspects for the treatment of cardiac diseases based on the diversity of functional controls on cardiac muscles: Mitochondrial ion channels and cardioprotection. *J Pharmacol Sci.* 2009;109:341–347.
- 38 Sanbandam N, Lopaschuk GD, Brownsey RW, Allard MF. Energy metabolism in the hypertrophied heart. *Heart Failure Rev.* 2002;7:161–173.
- 39 Agata N, Kato Y, Tanaka H, Shigenobu K. Differential effects of hypoxia on electrical and mechanical activities of isolated ventricular muscles from fetal and adult guinea pigs. *Gen Pharmacol.* 1994;25:15–18.

Short Communication

Involvement of the Na⁺/Ca²⁺ Exchanger in the Automaticity of Guinea-Pig Pulmonary Vein Myocardium as Revealed by SEA0400

Iyuki Namekata^{1,*}, Yayoi Tsuneoka¹, Akira Takahara¹, Hideaki Shimada¹, Takahiko Sugimoto¹, Kiyoshi Takeda¹, Midori Nagaharu¹, Koki Shigenobu¹, Toru Kawanishi², and Hikaru Tanaka¹

¹Department of Pharmacology, Toho University Faculty of Pharmaceutical Sciences, Funabashi, Chiba 274-8510, Japan

²Division of Drugs, National Institute of Health Sciences, Setagaya-ku, Tokyo 158-8501, Japan

Received June 21, 2008; Accepted March 19, 2009

Abstract. We examined the involvement of the Na⁺/Ca²⁺ exchanger in the automaticity of the pulmonary vein myocardium with a specific inhibitor, SEA0400. Action potentials were recorded from the myocardial layer of isolated guinea-pig pulmonary vein preparations, and Ca²⁺ transients were recorded from the cardiomyocytes. Spontaneous electrical activity was observed in 17.7% of the preparations, which was inhibited by either SEA0400 or ryanodine. In quiescent preparations, ouabain induced electrical activity and spontaneous Ca²⁺ transients, which were inhibited by SEA0400, as well as ryanodine. These results provide pharmacological evidence that the Na⁺/Ca²⁺ exchanger underlies the automaticity of the pulmonary vein myocardium.

Keywords: pulmonary vein myocardium, Na⁺/Ca²⁺ exchanger, automaticity

Pulmonary veins are considered to be involved in the initiation and maintenance of atrial fibrillation, one of the most frequent arrhythmias in clinical practice (1). Pulmonary veins contain a myocardial layer, whose electrical activity is considered to underlie their arrhythmogenic activity (2). The pulmonary vein myocardium has different electrophysiological properties from those of the working myocardium, including lower density of I_{K1} and a less negative resting membrane potential (3). The precise mechanisms of the pulmonary vein electrical activity as well as its pharmacological properties are now receiving attention as the basis to develop an effective therapeutic strategy against atrial fibrillation.

The Na⁺/Ca²⁺ exchanger (NCX) is involved in the physiological and pathophysiological regulation of Ca²⁺ concentration in the myocardium. It functions both in the forward (Ca²⁺ extrusion) and reverse (Ca²⁺ influx) modes, and its functional role may vary with the region and the condition of the myocardium (4, 5). The forward mode NCX activity (inward current) is the major pathway for Ca²⁺ extrusion from the cytoplasm and is also considered to be involved in the normal pacemaking of the rabbit sinoatrial node (6). It was postulated that the

Ca²⁺ released from the sarcoplasmic reticulum (SR) during the diastolic period is pumped out of the cell through the forward mode NCX, which generates an inward current that contributes to the diastolic depolarization of the pacemaker. Although it is possible that such a mechanism is involved in the automaticity of other myocardial regions including the pulmonary vein myocardium, pharmacological evidence is limited because of the lack of an NCX inhibitor with sufficient specificity.

SEA0400 {2-[4-[(2,5-difluorophenyl) methoxy] phenoxy]-5-ethoxyaniline} is a potent and selective inhibitor of NCX in cultured neurons, astrocytes, microglia, dog sarcolemmal vesicles, and cultured rat myocytes with negligible affinities towards other transporters, ion channels, and receptors (7). We have previously shown that SEA0400 is a specific inhibitor of NCX in the myocardium (8, 9). SEA0400 (1 μM), which inhibited the NCX current by more than 80%, had no effect on the Na⁺ current, L-type Ca²⁺ current, delayed rectifier K⁺ current, inwardly rectifying K⁺ current (8), and the Ca²⁺ sensitivity of contractile proteins (5). This was in contrast with the effects of KB-R7943, a compound that has been widely used as an NCX inhibitor; KB-R7943 inhibited all of the above mentioned currents with equal potency (8). Thus, SEA0400 was established as the first specific pharmacological tool to study the role of NCX

*Corresponding author. iyuki@phar.toho-u.ac.jp
Published online in J-STAGE on May 8, 2009 (in advance)
doi: 10.1254/jphs.08159SC

and was shown to be useful in studies on myocardial excitation-contraction mechanisms, regulation by autonomic transmitters, and ischemia-reperfusion injury (5, 10, 11). In the present study, we examined the effects of SEA0400 and ryanodine on the spontaneous and ouabain-induced electrical activity of the guinea-pig pulmonary vein myocardium to clarify the role of NCX in automaticity.

All experiments were approved by the Ethics Committee of Toho University Faculty of Pharmaceutical Sciences and performed in accordance with the Guiding Principles for the Care and Use of Laboratory Animals approved by The Japanese Pharmacological Society. Hearts with lungs were quickly removed from male or female Hartley guinea pigs (weight, 350–450 g). The pulmonary veins were separated from the atrium at the left atrium-pulmonary vein junction, and separated from the lungs at the ending of the pulmonary vein myocardial sleeves. Tubular pulmonary veins were cut open and pinned down endocardial side up on the bottom of the 20-ml recording chamber. The extracellular solution contained 118.4 mM NaCl, 4.7 mM KCl, 2.5 mM CaCl₂, 1.2 mM MgSO₄, 1.2 mM KH₂PO₄, 24.9 mM NaHCO₃, and 11.1 mM glucose (pH 7.4); it was gassed with 95% O₂–5% CO₂ and maintained at 36 ± 0.5°C. The low-sodium extracellular solution was prepared with the equimolar substitution of NaCl with LiCl so that the final Na⁺ concentration was 70 mM. Change to low-Na⁺ solution and return to normal solution were performed with superfused pulmonary-vein tissue preparations and an original flow-switching device; the time required for change of the solution was approximately 1 s.

Action potentials were recorded in pulmonary vein tissue preparations by standard microelectrode penetrations from the luminal side. The glass microelectrodes filled with 3 M KCl had resistances of 20–30 MΩ. The output of a microelectrode amplifier (MEZ8201; Nihon Kohden, Tokyo) with high input impedance and capacity neutralization was recorded and analyzed by an action potential analyzing system (Analog-Pro DMA and DSS type IV; Canopus, Tokyo). The action potential parameters: resting potential (RP); maximum diastolic potential (MDP); overshoot (OS); maximum rate of rise (\dot{V}_{\max}); action potential duration at 20%, 50%, and 90% repolarization (APD₂₀, APD₅₀, APD₉₀, respectively); and the slope of the depolarization phase were measured under electrical stimulation at 1 Hz.

Confocal microscopic analyses of the Ca²⁺ dynamics in isolated pulmonary-vein cardiomyocytes were performed with LSM 510 (Carl Zeiss, Jena, Germany) and procedures basically the same as those used for ventricular myocytes as previously described (12). After Langendorff perfusion of the heart with the pulmonary

veins attached and treatment with 1 mg/ml collagenase (YK-102; Yakult, Tokyo) for about 20 min, the pulmonary vein cardiomyocytes were isolated, treated with fluo-4/AM, and superfused with the extracellular solution of the following composition gassed with 100% O₂ at 36 ± 0.5°C: 143 mM NaCl, 5.4 mM KCl, 1.0 mM MgCl₂, 1.8 mM CaCl₂, 0.33 mM NaH₂PO₄, 5.5 mM glucose, and 5 mM HEPES. The cells were line scanned at a speed of line/960 μs. The excitation wavelength was 488 nm and fluorescence with wavelength above 505 nm was detected and analyzed.

SEA0400 was provided by Taisho Pharmaceutical Company, Ltd. (Saitama). Ryanodine and ouabain were purchased from Wako (Osaka) and Sigma (St. Louis, MO, USA), respectively. These compounds were dissolved in dimethyl sulfoxide (final concentration of 0.01%). All other chemicals used were of the highest commercially available quality. Data were expressed as the mean ± S.E.M. Statistical significance between means was evaluated by the paired *t* test or by the one-way repeated measures analysis of variance followed by Contrasts for mean values comparison or by Fisher's exact test; a *P* value less than 0.05 was considered significant.

Among the 141 isolated guinea-pig pulmonary vein preparations examined, 116 preparations showed no spontaneous activity. The action potential parameters of such quiescent preparations when driven at 1 Hz were RP: -71.4 ± 1.9 mV, MDP: -75.4 ± 1.5 mV, OS: 30.9 ± 1.5 mV, \dot{V}_{\max} : 135.6 ± 15.5 V/s, APD₂₀: 16.7 ± 2.0 ms, APD₅₀: 37.7 ± 2.8 ms, and APD₉₀: 92.9 ± 1.2 ms (*n* = 6). An obvious diastolic depolarization was observed, although the site of microelectrode penetration was not at the very center of the pacemaking region of the pulmonary vein myocardium. The slope of the diastolic depolarization was 9.5 ± 2.0 mV/s (*n* = 6). SEA0400 (1 μM) significantly shortened the action potential duration (APD₅₀ and APD₉₀) and decreased the slope of the diastolic depolarization without affecting other parameters. The action potential parameters after the application of SEA0400 were RP: -70.5 ± 1.6 mV, MDP: -73.7 ± 1.2 mV, OS: 30.7 ± 1.6 mV, \dot{V}_{\max} : 128.3 ± 15.8 V/s, APD₂₀: 15.3 ± 1.8 ms, APD₅₀: 33.1 ± 2.2 ms, APD₉₀: 87.6 ± 2.1 ms, and the slope of the depolarization phase: 6.3 ± 1.1 mV/s (*n* = 6).

The other 25 preparations showed spontaneous electrical activity (17.7%, Fig. 1A). After confirming that the spontaneous activity persisted for 30 min, drugs were applied and the effects were observed for 30 min. SEA0400 (1 μM) prolonged the cycle length of the spontaneous action potential followed by complete suppression within 10 min (Fig. 1Aa, Table 1). Concerning the specificity of SEA0400, it was reported that

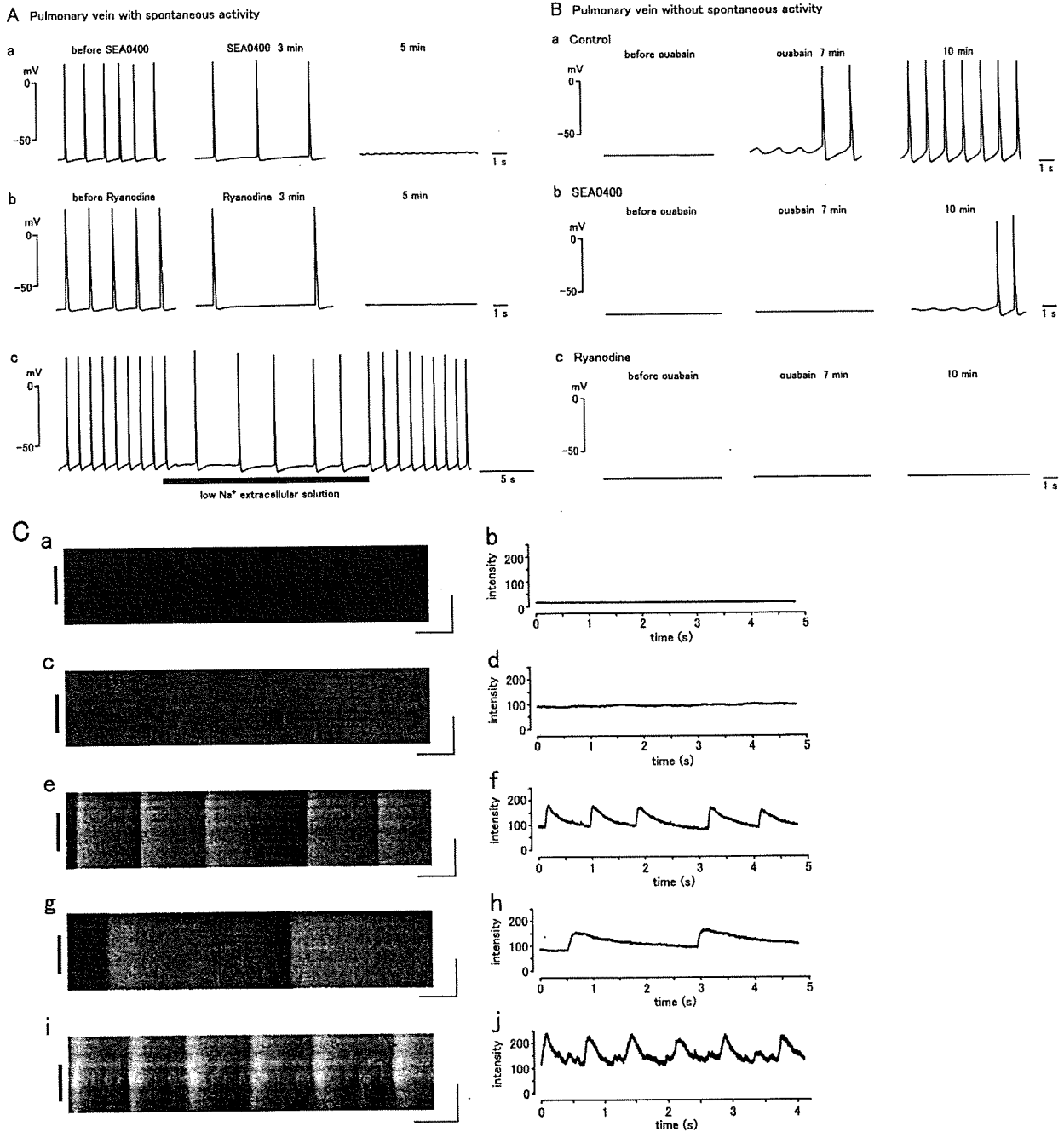


Fig. 1. Pharmacological properties of electrical activity and intracellular Ca²⁺ transient in pulmonary vein myocardia. **A:** Inhibition by SEA0400, ryanodine, and low-Na⁺ extracellular solution of the spontaneous activity in pulmonary vein myocardial tissue. Typical action potential traces showing the effects of 1 μ M SEA0400 (a), 0.1 μ M ryanodine (b), and rapid change of the extracellular solution to low-Na⁺ solution (c). **B:** Inhibition by SEA0400 and ryanodine of the ouabain-induced electrical activity in pulmonary vein myocardial tissue. Typical action potential traces showing the effect of 1 μ M ouabain on a quiescent preparation in the absence (a) or presence of 1 μ M SEA0400 (b) or 0.1 μ M ryanodine (c). **C:** Confocal line-scan images of intracellular Ca²⁺ (a, c, e, g, i) and the time course of fluorescence intensity (b, d, f, h, j) in isolated pulmonary-vein myocardial cells. In a quiescent cell (a, b), ouabain induced an elevation of cytoplasmic Ca²⁺ (c, d) followed by generation of spontaneous Ca²⁺ transients (e, f). Further application of SEA0400 reduced the frequency of Ca²⁺ transients (g, h) and eventually completely inhibited spontaneous activity. In another cell, the Ca²⁺ sparks induced by ouabain, as well as Ca²⁺ transients, could be detected in the scanning line (i, j). The scanning line was placed along the longitudinal axis of the cardiomyocyte. Horizontal and vertical scale bars in a, c, e, g, and i indicate 500 ms and 10 μ m, respectively; and the bars on the left side indicate the regions quantified.

Table 1. Inhibition by SEA0400 and ryanodine of pulmonary vein spontaneous activity

	Frequency (Hz)			Average of cessation time (min)	Cessation at 10 min (%)
	0 min	5 min	10 min		
Control	1.1 ± 0.2	1.1 ± 0.2	1.2 ± 0.3	—	0/7 (0%)
SEA0400 (1 μM)	1.1 ± 0.5	0.6 ± 0.6	0 [†]	5.7 ± 1.5	6/6 (100%)*
Ryanodine (0.1 μM)	0.9 ± 0.1	0.6 ± 0.2 [†]	0.2 [†]	6.2 ± 1.5	5/6 (83.3%)*

Effects of SEA0400 or ryanodine on the spontaneous activity of pulmonary vein preparations are summarized in this table. SEA0400 or ryanodine was applied to spontaneously firing preparations. The frequency was sampled at 5 min because the drugs caused cessation in most of the preparations at 10 min. Asterisks indicate significant differences from the control values as evaluated by Fisher's exact test (* $P < 0.05$). Daggers indicate significant differences from the corresponding values at 0 min as evaluated by one-way repeated measures analysis of variance followed by Contrasts for mean values comparison ([†] $P < 0.05$).

Table 2. Inhibition by SEA0400 and ryanodine of the ouabain-induced pulmonary vein electrical activity

	Incidence at 30 min (%)	Latency (min)	Frequency at 15 min (Hz)
Control	13/15 (86.7%)	7.0 ± 0.9	4.8 ± 0.4
SEA0400 (1 μM)	7/15 (46.7%)*	9.8 ± 1.2	3.5 ± 0.5
SEA0400 (10 μM)	2/11 (18.2%)*	13.1 ± 3.1	0.2
Ryanodine (0.1 μM)	0/7 (0%)*		

Ouabain (1 μM) was applied to quiescent pulmonary vein preparations in the presence of vehicle (control), SEA0400, or ryanodine; and the incidence of electrical activity at 30 min is summarized. For the preparations in which ouabain induced electrical activity, the latency before the first firing and the frequency at 15 min are summarized; it took an average of 7–13 min before activity was induced. SEA0400 or ryanodine was present from 30 min before the application of ouabain. Asterisks indicate significant differences from the control values as evaluated by Fisher's exact test (* $P < 0.05$).

SEA0400 depresses Ca^{2+} transients in NCX1-knockout mouse (13). Although such non-specific effects of SEA0400 has not been reported in normal animals, the possibility that the compound is acting through mechanisms other than NCX inhibition can not be totally excluded. Thus, we intended to inhibit forward-mode NCX activity with low Na^+ extracellular solution. Changing the extracellular solution to low Na^+ solution caused slowing of the spontaneous electrical activity within a few seconds and this recovered after return to normal solution (Fig. 1Ac); the frequency of the spontaneous activity under normal and low- Na^+ condition was 1.2 ± 0.1 and 0.6 ± 0.1 ($P < 0.05$, $n = 6$), respectively. Ryanodine (0.1 μM) suppressed spontaneous activity in most of the preparations (Fig. 1Ab, Table 1).

In the pulmonary vein preparations without spontaneous activity, 1 μM ouabain induced membrane potential oscillations, leading to the repetitive generation of action potentials (Fig. 1Ba). Pretreatment with SEA0400 suppressed the ouabain-induced electrical activity in a concentration dependent manner (Fig. 1Bb, Table 2). Concerning the preparations in which ouabain-induced electrical activity persisted in the presence of SEA0400, the latency was longer and the frequency was lower than those in the preparations treated with ouabain alone (Table 2). In the presence of ryanodine (0.1 μM),

ouabain (1 μM) did not induce electrical activity (Fig. 1Bc, Table 2).

To clarify the effect of ouabain and SEA0400 on intracellular Ca^{2+} , the drugs were applied to isolated pulmonary-vein myocardial cells loaded with the fluorescent Ca^{2+} indicator, fluo-4, under line-scan mode confocal microscopy (Fig. 1C). In quiescent pulmonary-vein cardiomyocytes (Fig. 1Ca, b), ouabain (1 μM) induced an increase in cytoplasmic Ca^{2+} concentration (Fig. 1Cc, d) and generation of spontaneous Ca^{2+} transients (Fig. 1Ce, f); the basal fluorescence intensity of the cells after the induction of spontaneous activity was $281.8 \pm 60\%$ ($n = 6$) of intensity under quiescence. Further application of SEA0400 decreased the frequency of the Ca^{2+} transients and eventually completely inhibited the Ca^{2+} transients without decreasing the diastolic Ca^{2+} level (Fig. 1Cg, h); the fluorescence was $100.8 \pm 2.1\%$ ($n = 6$) of the value before application of SEA0400. In some cells, the induction by ouabain (1 μM) of Ca^{2+} sparks, as well as spontaneous Ca^{2+} transients, could be detected within the scanning line (Fig. 1Ci, j). Ryanodine (0.1 μM) completely inhibited Ca^{2+} transients ($n = 6$).

In the present study, about 18% of the guinea-pig pulmonary vein preparations showed spontaneous activity (Fig. 1A); the incidence was increased by ouabain. Ouabain has been used as a pharmacological

tool to induce intracellular Ca^{2+} overload through inhibition of the Na^+/K^+ ATPase (14), although other mechanisms of action have also been postulated (15). Increased cellular Ca^{2+} load can cause elevation of the diastolic Ca^{2+} level and/or induce spontaneous Ca^{2+} release from the SR. These would accelerate the diastolic depolarization through enhancement of the forward-mode NCX and thereby elicit electrical activity. Our present results that ouabain induced elevation of diastolic Ca^{2+} level and induced Ca^{2+} sparks and that ouabain-induced electrical activity was inhibited by ryanodine and SEA0400 suggest that this is indeed the case. The spontaneous electrical activity was inhibited by ryanodine and SEA0400 and also by low Na^+ extracellular solution. These results indicated that for both the ouabain-induced and spontaneous electrical activities, the basic mechanism is activation of the forward-mode NCX by Ca^{2+} released from the SR. Acceleration of late repolarization (reduction of APD_{50} and APD_{90}) and reduction of the slope of diastolic depolarization by SEA0400 supports the view that Ca^{2+} extrusion through forward mode NCX occurs during the repolarization phase and the diastolic depolarization phase.

Ouabain, at a concentration of $1 \mu\text{M}$, induced electrical activity in the guinea-pig pulmonary vein myocardium (Fig. 1B, Table 2). This concentration of ouabain did not induce electrical activity in the ventricular myocardium (11). The pulmonary vein myocardium is reported to have different electrophysiological properties from those of the working myocardium such as lower density of $\text{I}_{\text{K}1}$ and a less negative resting membrane potential (3). The resting membrane potential of the guinea-pig pulmonary vein myocardial cells in the present study was -71.4 mV , which was less negative than that of the guinea-pig atria and ventricle (-78 to -85 mV , ref. 16). The smaller contribution of $\text{I}_{\text{K}1}$ around the resting membrane potential would allow underlying depolarizing mechanisms to contribute to diastolic depolarization, leading to the generation of spontaneous action potentials in the pulmonary vein myocardium. In the guinea-pig ventricular myocardium, SEA0400 ($1 \mu\text{M}$) decreased the incidence of ouabain-induced arrhythmic contraction from 73% to 46% (11). This potency of SEA0400 to inhibit automaticity is similar to that in the pulmonary vein preparations (87% to 47%, Table 2). This suggests that the depolarizing mechanisms involving the forward-mode NCX is intrinsically present in both the ventricular and pulmonary vein myocardium, but manifests itself as automaticity preferentially in the pulmonary vein because of the limited ability to maintain the resting membrane potential.

The pulmonary vein is considered to be a source of ectopic electrical activity that leads to paroxysms of

atrial fibrillation (2). Abnormalities in intracellular Ca^{2+} homeostasis induced by factors such as increased mechanical stretch has been suggested to underlie the generation of ectopic activity in the pulmonary vein (17). The Ca^{2+} influx through stretch-activated cation channels may load the SR above its capacity and cause spontaneous focal Ca^{2+} release from the SR. This would lead to the generation of arrhythmias through forward-mode NCX activity. The present results with SEA0400 indicate that Ca^{2+} overload-induced electrical activity in the pulmonary vein myocardium can be reduced by NCX inhibition. Thus, NCX inhibition may be an effective therapeutic strategy for the treatment of atrial fibrillation of pulmonary vein origin. Extension of the present study with experiments, such as direct recording from the center of the pacemaking region of the pulmonary vein myocardium, simultaneous recording of Ca^{2+} concentration and membrane potential, and evaluation of the effect of drugs in clinical use, would lead to a deeper understanding of the pulmonary vein automaticity and its therapeutic significance.

In conclusion, the present results provide pharmacological evidence that the forward-mode NCX activated by Ca^{2+} released from the SR is involved in the automaticity of the pulmonary vein myocardium.

Acknowledgments

This study was in part performed as a part of the project "Research on the molecular mechanisms of appearance of age-related diseases by failure of cell function control system, and their prevention and treatment" by the "Research Center for Aging and Age related Diseases" established in the Toho University Faculty of Pharmaceutical Sciences. This study was supported in part by Grants-in-Aid from the Ministry of Education, Culture, Sports, Science, and Technology of Japan to I.N. (#20890233), A.T. (#19590532), and H.T. (#18590243). It was also supported in part by a Grant-in-Aid for Research on Publicly Essential Drugs and Medical Devices to K.S. and T.K. from the Japan Health Science Foundation.

References

- Haïssaguerre M, Jaïs P, Shah DC, Takahashi A, Hocini M, Quiniou G, et al. Spontaneous initiation of atrial fibrillation by ectopic beats originating in the pulmonary veins. *N Engl J Med.* 1998;339:659–666.
- Chen YJ, Chen SA, Chang MS, Lin CI. Arrhythmogenic activity of cardiac muscle in pulmonary veins of the dog: implication for the genesis of atrial fibrillation. *Cardiovasc Res.* 2000;48:265–273.
- Ehrlich JR, Cha TJ, Zhang L, Chartier D, Melnyk P, Hohnloser SH, et al. Cellular electrophysiology of canine pulmonary vein cardiomyocytes: action potential and ionic current properties. *J Physiol.* 2003;551:801–813.
- Bers D, Pogwizd S, Schlotthauer K. Upregulated $\text{Na}^+/\text{Ca}^{2+}$ exchange is involved in both contractile dysfunction and

- arrhythmogenesis in heart failure. *Basic Res Cardiol.* 2002;97:136–142.
- 5 Tanaka H, Namekata I, Takeda K, Kazama A, Shimizu Y, Moriwaki R, et al. Unique excitation-contraction characteristics of mouse myocardium as revealed by SEA0400, a specific inhibitor of $\text{Na}^+\text{-Ca}^{2+}$ exchanger. *Naunyn Schmiedebergs Arch Pharmacol.* 2005;371:526–534.
 - 6 Maltsev V, Vinogradova T, Lakatta E. The emergence of a general theory of the initiation and strength of the heartbeat. *J Pharmacol Sci.* 2006;100:338–369.
 - 7 Matsuda T, Arakawa N, Takuma K, Kishida Y, Kawasaki Y, Sakaue M, et al. SEA0400, a novel and selective inhibitor of the $\text{Na}^+\text{-Ca}^{2+}$ exchanger, attenuates reperfusion injury in the in vitro and in vivo cerebral ischemic models. *J Pharmacol Exp Ther.* 2001;298:249–256.
 - 8 Tanaka H, Nishimaru K, Aikawa T, Hirayama W, Tanaka Y, Shigenobu K. Effect of SEA0400, a novel inhibitor of sodium-calcium exchanger, on myocardial ionic currents. *Br J Pharmacol.* 2002;135:1096–1100.
 - 9 Namekata I, Kawanishi T, Iida-Tanaka N, Tanaka H, Shigenobu K. Quantitative fluorescence measurement of cardiac $\text{Na}^+\text{-Ca}^{2+}$ exchanger inhibition by kinetic analysis in stably transfected HEK293 cells. *J Pharmacol Sci.* 2006;101:356–360.
 - 10 Namekata I, Nakamura H, Shimada H, Tanaka H, Shigenobu K. Cardioprotection without cardiosuppression by SEA0400, a novel inhibitor of $\text{Na}^+\text{-Ca}^{2+}$ exchanger, during ischemia and reperfusion in guinea-pig myocardium. *Life Sci.* 2005;77:312–324.
 - 11 Tanaka H, Shimada H, Namekata I, Kawanishi T, Shigenobu K. Involvement of the $\text{Na}^+\text{-Ca}^{2+}$ exchanger in ouabain-induced inotropy and arrhythmogenesis in guinea-pig myocardium as revealed by SEA0400. *J Pharmacol Sci.* 2007;103:241–246.
 - 12 Namekata I, Yamagishi R, Kato Y, Nakamura R, Tanaka H, Shigenobu K. Propagation of normal and abnormal cytoplasmic Ca^{2+} oscillations into the cell nucleus in cardiomyocytes. *Bioimages.* 2004;12:61–69.
 - 13 Reuter H, Henderson SA, Han T, Matsuda T, Baba A, Ross RS, et al. Knockout mice for pharmacological screening: testing the specificity of $\text{Na}^+\text{-Ca}^{2+}$ exchange inhibitors. *Circ Res.* 2002;91:90–92.
 - 14 Bers D. Cardiac inotropy and Ca mismanagement cardiac inotropy. In: Bers D editor. *Excitation-contraction coupling and cardiac contractile force.* 2nd ed. Dordrecht: Kluwer Academic Publishers; 2001. p. 273–331.
 - 15 Wasserstrom JA, Aistrup GL. Digitalis: new actions for an old drug. *Am J Physiol Heart Circ Physiol.* 2005;289:H1781–H1793.
 - 16 Matsuda T, Takeda K, Ito M, Yamagishi R, Tamura M, Nakamura H, et al. Atria selective prolongation by NIP-142, an antiarrhythmic agent, of refractory period and action potential duration in guinea pig myocardium. *J Pharmacol Sci.* 2005;98:33–40.
 - 17 Scoote M, Williams AJ. Myocardial calcium signalling and arrhythmia pathogenesis. *Biochem Biophys Res Commun.* 2004;322:1286–1309.

Division of Drugs¹, National Institute of Health Sciences; Bruker Optics K.K.², Tokyo; TDDS Laboratory³, Hisamitsu Pharmaceutical Co Inc, Ibaraki; Tokyo Metropolitan Industrial Technology Research Institute⁴, Tokyo, Japan

Chemical mapping of tulobuterol in transdermal tapes using Microscopic Laser Raman Spectroscopy

T. SAKAMOTO¹, T. MATSUBARA², D. SASAKURA², Y. TAKADA³, Y. FUJIMAKI⁴, K. AIDA³, T. MIURA², T. TERAHARA³, N. HIGO³, T. KAWANISHI¹, Y. HIYAMA¹

Received July 29, 2008, accepted August 5, 2008

Tomoaki Sakamoto, Ph.D., National Institute of Health Sciences, 1-18-1, Kami-yoga, Setagaya-ku, Tokyo 158-8501, Japan
tsakamot@nihs.go.jp

Pharmazie 64: 166–171 (2009)

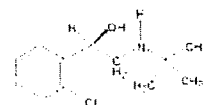
doi: 10.1691/ph.2008.8217

Microscopic Laser Raman Spectroscopy and Mapping (MLRSM) technique was used to investigate the distribution of tulobuterol (TBR) crystals in transdermal tapes. TBR is one of suitable compounds for the transdermal pharmaceuticals because it has high permeability into skin. In case of TBR transdermal tapes, some commercial products also contain TBR crystals in order to control a release rate from a matrix. Therefore, the presence of TBR crystals in the matrix is a critical factor for quality assurance of this type of TDDS tapes. The model tapes prepared here employed two kinds of matrices, i.e., rubber or acrylic, which are generally used for transdermal pharmaceuticals. TBR crystals in the matrix were observed by MLRSM. Accurate observation of the distribution of TBR in the tapes was achieved by creating a Raman chemical map based on detecting unique TBR peak in each pixel. Moreover, differences in the growth of TBR crystals in the two kinds of matrices were detected by microscopic observation. MLRSM also enabled the detection of TBR crystals in commercial products. The present findings suggest that Raman micro-spectroscopic analysis would be very useful for verifying and/or assessing the quality of transdermal pharmaceuticals in development, as well as for manufacturing process control.

1. Introduction

Tulobuterol (TBR) transdermal tapes are applied in cases of bronchial asthma as a bronchodilator (β_2 -blocker). TBR suitable for use in transdermal drug delivery because it has high permeability into the keratin layer (Uematsu et al. 1993). TBR pharmaceutical products with a Transdermal Drug Delivery System (TDDS) have advantages such as eliminating the side effects including abdominal pain and appetite loss (Iikura et al. 1995), and maintaining effective blood TBR levels for approximately 24 h (Horiguchi et al. 2004). The release rate of TBR from the matrix is controlled by the formation of TBR crystals. The crystallization of TBR has the possibility of influencing the TBR blood level profile. Therefore, it is necessary to characterize not only the release rate of TBR from a matrix, but also to characterize its crystallinity in dosage form in the matrix. *In vitro* penetration testing using stripped animal skin and *in vitro* release testing have been used to evaluate transdermal pharmaceuticals in terms of penetration and release. Because these evaluation methods show only one of several alternative physicochemical parameters (e.g., release rate, rate of penetration rate of an active substance, etc.), it has remained difficult to clarify the chemical status and quality of transdermal pharmaceuticals. In case of transdermal tapes containing an active drug as crystals in a matrix, the active drug is slowly re-

leased from the matrix into the keratin layer, as crystals will gradually dissolve in a matrix. Therefore, the crystallization of TBR is an important quality parameter. However, evaluation of the correlation of release rates between animal skin and human skin using *in vitro* penetration testing of animal skin has also remained difficult. Therefore, it has become desirable to develop analytical methods of both microscopically and chemically detecting and observing crystals of active drugs in a matrix.



Tulobuterol (TBR)

Laser Raman spectroscopy is a method of spectroscopic analysis of spectra of Raman scattered light obtained by exposure of a sample to a laser. Raman spectroscopy has been used for the identification and quantification of polymorphs (Deely et al. 1991; Falcon et al. 2004; Ferrari et al. 2004; Findlay et al. 1998; Hu et al. 2005; Langkilde et al. 1997; Ono et al. 2004; Schöll et al. 2006; Starbuck et al. 2002; Wang et al. 2000; Murphy et al. 2005) and for monitoring the crystallization process (Taylor et al. 1998;